EUROPEAN ORGANIZATION FOR NUCLEAR RESEARCH

CERN-EP/87-121
10 July 1987

A MEASUREMENT OF THE INCLUSIVE π^0 AND η PRODUCTION CROSS-SECTIONS AT HIGH p_T in $p\bar{p}$ AND pp COLLISIONS AT $\sqrt{s}$ = 24.3 GeV

CERN[1)], Lausanne[2)], Michigan[3)], Rockefeller[4)]
(UA6) Collaboration

J. Antille[2)], S. Baumann[2)], A. Bernasconi[2)], R.E. Breedon[4)], L. Camilleri[1)], R.L. Cool[4)], P.T. Cox[4)], L. Dick[1)], E.C. Dukes[1,3)], M. Duro[3,4)], B. Gabioud[2)], F. Gaille[1,2)], P. Giacomelli[4)], J.B. Jeanneret[1)], C. Joseph[2)], W. Kubischta[1)], J.F. Loude[2)], E. Malamud[2,*)], C. Morel[2)], O.E. Overseth[3)], J.L. Pages[2)], J.P. Perroud[2)], P. Petersen[4)], D. Ruegger[2)], R.W. Rusack[4)], G.R. Snow[4,3)], G. Sozzi[2)], D. Steiner[2)], M.T. Tran[2)], A. Vacchi[1,4)], G. Valenti[3,**)] and G. von Dardel[1)].

ABSTRACT

Inclusive π^0 and η production at large transverse momentum were studied in $p\bar{p}$ and pp interactions at $\sqrt{s}$ = 24.3 GeV. The experiment was performed using an internal molecular-hydrogen gas-jet target in the CERN $p\bar{p}$ Collider. No significant differences between production in $p\bar{p}$ and pp were observed in the transverse momentum range $2.5 < p_T < 5.1$ GeV/c.

(Submitted to Physics Letters B)

*) Permanent address: Fermilab, Batavia, Il 60510, USA.
**) Also at: INFN Bologna, Italy.

1. INTRODUCTION

Single-particle production at high transverse momentum (p_T) has been extensively studied in recent years [1,2]. High-p_T particles produced in hadronic collisions are thought to arise from the interaction of two partons in the colliding hadrons. The scattered partons subsequently fragment into hadrons, one of which is the observed high-p_T particle. A particle of sufficiently high p_T will be the leading particle in the fragmentation and thus its direction is likely to be closely related to the direction of the parent parton. Furthermore, the relative abundances of different particles produced should yield information on the importance of different parton combinations in the scattering process. According to this model, the production of high-p_T particles in $p\bar{p}$ and pp interactions may be different owing to the different quark structures of the proton and the antiproton. The UA6 Collaboration has embarked on a programme to study the various high-p_T phenomena in $p\bar{p}$ and pp collisions, with emphasis on direct photons. This paper presents data on the inclusive production of high-p_T π^0 and η mesons from the first UA6 run in $p\bar{p}$ at $\sqrt{s}$ = 24.3 GeV, and compares them with pp data at the same $\sqrt{s}$, collected in the same detector and with the same trigger. This allows a direct comparison of $p\bar{p}$ and pp interactions to be made, while minimizing systematic effects.

2. THE APPARATUS

Experiment UA6 is located in a 12 m straight section of the CERN Super Proton Synchrotron (SPS). The detector [3-6], shown in fig. 1, consists of a molecular-hydrogen jet followed by a double-arm spectrometer. Each arm covers polar angles from 20 to 100 mrad in the laboratory system and 70° in azimuth for a total acceptance of 1.8 sr in the $p\bar{p}$ (or pp) centre-of-mass system. An arm consists of: five multiwire proportional chambers (PC1-PC5), two in front of, and three behind, a 2.3 T·m dipole magnet; an ionization chamber (dE/dx); a Li/Xe transition radiation detector; and an electromagnetic calorimeter.

The jet target consists of a stream of pure hydrogen clusters, each cluster containing about 10^5 molecules, which traverses the SPS beams. The maximum jet density of 4×10^{14} protons/cm^3 provides an average luminosity of 5.5×10^{29} cm^{-2}s^{-1} for a typical number of 4×10^{10} stored antiprotons. (Each antiproton traverses the jet at the SPS revolution frequency of 43.4 kHz.) The pp luminosity was an order of magnitude higher owing to the larger number of stored protons. The jet density is sufficiently low that particles produced in the interaction have a very small probability of re-interacting. The small interaction volume is defined by the intersection of the jet with the $\bar{p}$ (p) beam. Its dimensions are given by the cross-section of the jet, 8 mm along the beam and 3 mm transverse to it, and by the thickness of the SPS beams, typically less than 1 mm.

The luminosity was determined, to within $\pm 5\%$, from the rate of elastic $p\bar{p}$ (or pp) events. This rate was continuously monitored by a set of solid-state counters (located at 90° in the laboratory system) in which the recoil proton from the jet was detected.

The two electromagnetic calorimeters [5] are of the lead/proportional-tube type. Each calorimeter consists of 30 lead plates, each 0.8 radiation length (r.l.) thick, interleaved with alternating layers of vertical and horizontal tubes of 1 cm transverse dimension and 0.5 cm thickness. The tubes are filled with a mixture of Ar (90%) + CO_2 (10%) and operated at a gas amplification of 10^3. The calorimeter is divided into three identical modules of 8 r.l. each. Located between the first and the second modules is a hodoscope of seven horizontal scintillator counters used for triggering. The analogue signals of the proportional tubes directly behind one another were summed within a module. This preserves the good lateral segmentation of the calorimeter (essential for γ/π^0 discrimination) and still provides three longitudinal samplings for electromagnetic showers. The position resolution for electromagnetic showers was found to be 3.5 mm at 10 GeV, improving to 1.5 mm at 75 GeV. Test-beam results showed that the calorimeter response to electrons in the energy range 10 to 100 GeV is linear, and that the energy resolution is $\sigma(E)/E = 0.33/\sqrt{E}$ (E in GeV). The electronic gain of each channel was determined using test pulses. Off line, the overall energy scale of the calorimeter was determined and adjusted on a run-to-run basis by centring the π^0 mass peak (fig. 2) at its known value. (A run of 30,000 triggers corresponded to about 1 hour of data-taking). Before adjustment, the energy scale was found to vary by $\pm 5\%$.

Both the $\bar{p}$- and the p-beam bunches cross the jet during Collider operation, albeit at different times and in different directions; therefore, switching from the study of $p\bar{p}$ interactions to the study of pp interactions involves rotating the whole apparatus by 180°.

3. DATA-TAKING AND ANALYSIS

The $p\bar{p}$ data come from an integrated luminosity of 43 nb^{-1} collected in 1984. The pp data were collected in 1986 after rotating the apparatus. A fraction of these data (40 nb^{-1}) were taken with the same trigger as that for the $p\bar{p}$ data in order to allow a direct comparison to be made.

The trigger used the scintillator hodoscopes situated 8 r.l. deep in the calorimeters, and thus sensitive on the average to the peak of electromagnetic showers initiated in the calorimeter. The signal from each of the seven horizontal counters per arm was separately discriminated at a threshold corresponding to $p_T \approx 1$ GeV/c.

In the off-line analysis, the pulse-height information from each tube was first converted to energy. Individual electromagnetic showers in the calorimeter were identified by clustering the detected energy. Clusters of neighbouring tubes containing energy above a threshold (30 MeV) were found in the horizontal (H) and vertical (V) views separately, and in each of the modules. The clusters were associated from module-to-module when a line through the cluster centroids extrapolated to the jet target. A cluster in the H view was then matched with a cluster in the V view if the corresponding partial energies were approximately equal, after allowing for the expected loss of energy in the lead between neighbouring H and V views.

4. π^0 and η PRODUCTION

The invariant mass of each pair of clusters found in the same calorimeter was calculated, assuming each cluster was due to a photon originating at the target. A typical mass distribution, from events in $p\bar{p}$ collisions, for pairs of clusters having a net $p_T > 2.5$ GeV/c, is shown in fig. 2. Clear peaks from the two-photon decays of π^0 and η mesons are seen. The π^0 and η candidates were chosen to be those in the mass range 0.0 to 0.2 GeV/c^2 and 0.45 to 0.65 GeV/c^2, respectively. To estimate the background under the peaks, the regions containing these mass intervals were each fitted to a Gaussian superimposed on a linear background. The insert in fig. 2 shows the result of such a fit in the region of the η peak. In this way approximately 10% of the combinations in the π^0 mass interval and 50% of those in the η mass interval were estimated to be background. The widths of the peaks, 18 MeV/c^2 for the π^0 and 35 MeV/c^2 for the η, are consistent with those expected from the energy and position resolutions of the calorimeter.

The invariant cross-sections were calculated from the numbers of π^0's and η's remaining after the background subtraction, using the measured luminosity and correcting for the trigger efficiency, geometrical acceptance of the detector, and efficiency of the off-line analysis. Only clusters with energy above 7 GeV were used for these calculations, in order to ensure good detection efficiency.

The overall acceptance was estimated using a Monte Carlo simulation. Candidate π^0 and η events were generated and passed through a simulation of the geometry of the detector, including the trigger hodoscope. The energies of the decay photons were distributed in the tubes of the simulated calorimeter according to shower-energy distributions measured for photons reconstructing to π^0's in the data themselves. The generated events were then passed through the off-line analysis and the acceptance obtained as a function of p_T.

The resulting invariant cross-section for inclusive π^0 production in $p\bar{p}$ collisions at $\sqrt{s}$ = 24.3 GeV is shown in fig. 3 as a function of p_T. Only statistical errors are shown. The uncertainty in the p_T scale is estimated to be $\pm 1.5\%$, and the normalization uncertainty is $\pm 7\%$, with about equal contributions from the uncertainty in the luminosity and in the value of the acceptance from the Monte Carlo.

The ratio of the invariant cross-section for π^0 production in $p\bar{p}$ collisions to that obtained in pp collisions is shown in fig. 4, in the range $2.5 < p_T < 5.1$ GeV/c. In this range the ratio is consistent with unity. The weighted average of the values is 0.965 ± 0.039, with a χ^2 of 4.8 for 4 degrees of freedom (d.o.f.). The data are also in good agreement with a measurement of π^0 production in pp collisions at $\sqrt{s} = 23.8$ GeV [7].

The ratio of η to π^0 cross-sections as a function of p_T for both $p\bar{p}$ and pp interactions is presented in fig. 5. This ratio is seen to be constant as a function of p_T. The weighted average of the $p\bar{p}$ data points is 0.458 ± 0.046, with a χ^2 of 1.5 for 3 d.o.f.; for the pp points it is 0.482 ± 0.040, with a χ^2 of 0.4 for 3 d.o.f. No difference in this ratio is seen between $p\bar{p}$ and pp collisions. The value of about 0.5 is in agreement with results obtained by several other experiments at lower and higher $\sqrt{s}$ [8-11].

The absence of differences between $p\bar{p}$ and pp interactions in π^0 and η production in this p_T range, already noted at the CERN Intersecting Storage Rings [11, 12], indicates that terms present in $p\bar{p}$ interactions and not in pp interactions, such as (Valence) $q\bar{q}$ annihilation, are not dominant in this reaction and kinematic domain.

Acknowledgements

We wish to thank the CERN PS and SPS Divisions for their magnificent achievement in operating the antiproton source and the SPS $p\bar{p}$ Collider. We also thank the EP and SPS Divisions for their extensive support during both the installation and the running stages of UA6. Finally, we gratefully acknowledge the dedicated technical support of R. Frei, R. Gros, J.P. Hertig, W. Huta, A. Kupferschmid, S. Manashe, G.R. Moser and H. Schick, and the secretarial help of M.-A. Huber.

REFERENCES

[1] P. Darriulat, Ann. Rev. Nucl. Sci. 30 (1980) 159.

[2] D. Treille, Proc. Int. Europhysics Conf. on High-Energy Physics, Bari, 1985, L. Nitti and G. Preparata, eds. (Laterza, Bari, 1985), p. 793.

[3] G. Valenti, Proc. 5th Topical Workshop on Proton-Antiproton Collider Physics, M. Greco, ed. (World Scientific, Singapore, 1985), p. 534.

[4] A. Vacchi, Proc. Wire Chamber Conference, Vienna, 1986 [Nucl. Instrum. Methods A252 (1986) 498].

[5] G. Snow, Proc. Gas Sampling Calorimetry Workshop II, FNAL, Batavia, 1985 (US Government Printing Office, 1986) p. 174.

[6] J. Antille et al., Nucl. Instrum. Methods 217 (1983) 327.

[7] C. De Marzo et al. A measurement of π^0 production at large transverse momentum in π^+p, π^-p, and pp collisions at 300 GeV/c, Max-Planck Institute preprint, MPI-PAE/EXP.EL.169 (1986).

[8] G.J. Donaldson et al., Phys. Rev. Lett. 40 (1978) 684.

[9] F.W. Büsser et al., Phys. Lett. 55B (1975) 232.

[10] C. Kourkoumelis et al., Phys. Lett. 84B (1979) 277.

[11] T. Åkesson et al., Phys. Lett. 158B (1985) 282.

[12] A.L.S. Angelis et al., Nucl. Phys. B263 (1986) 228.

FIGURE CAPTIONS

Fig. 1: The UA6 apparatus

Fig. 2: A typical invariant mass distribution of all two cluster combinations in the same calorimeter. The insert shows a typical fit to the η-mass region.

Fig. 3: Invariant differential cross-section as a function of p_T for inclusive π^0 production in pp at $\sqrt{s}$ = 24.3 GeV.

Fig. 4: The ratio of the invariant cross-sections for π^0 production in $p\bar{p}$ collisions and in pp collisions as a function of p_T.

Fig. 5: The ratio of η to π^0 cross-sections as a function of p_T for $p\bar{p}$ and pp interactions.

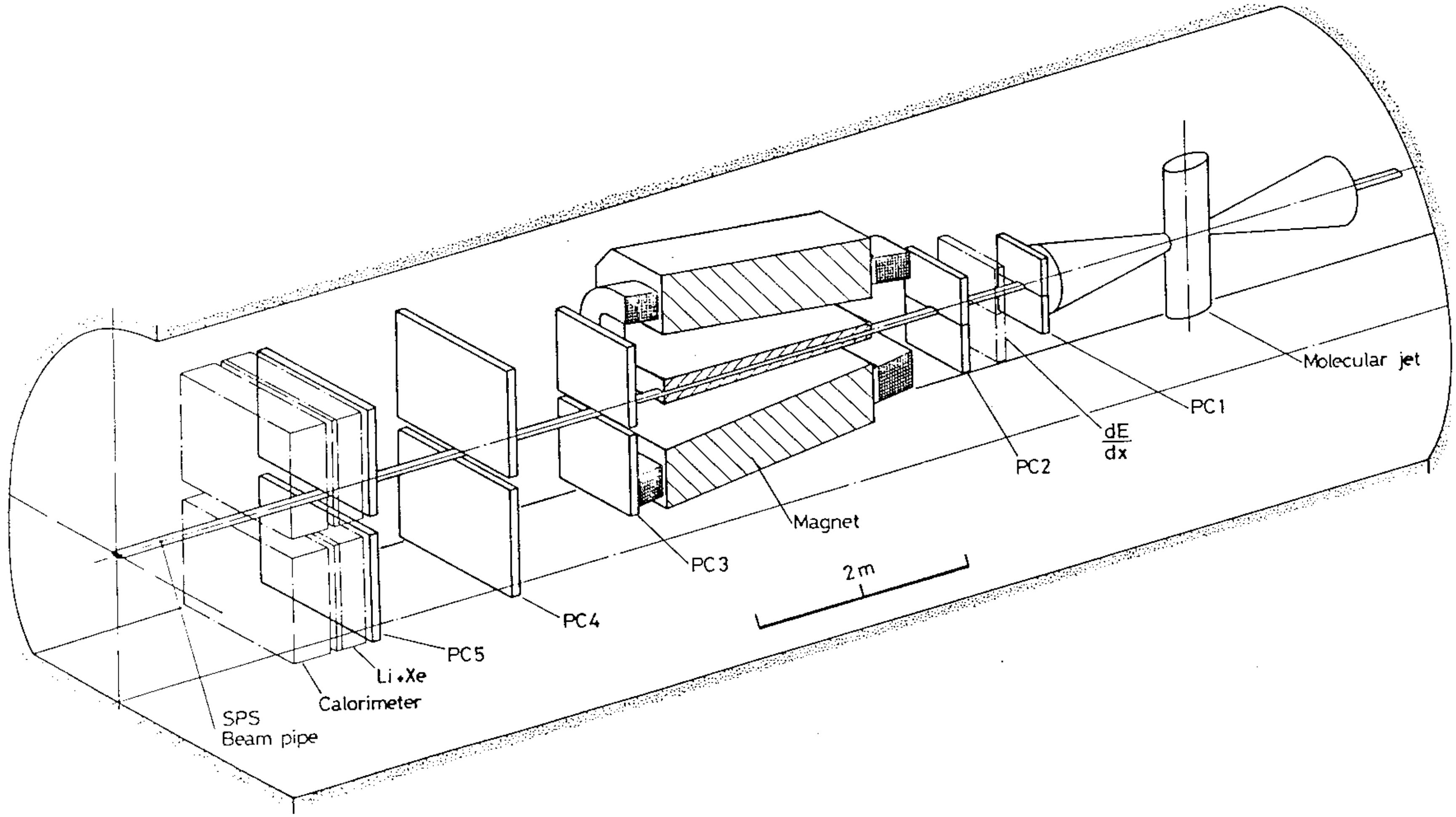
Molecular jet
PC1
dE/dx
PC2
Magnet
PC3
2 m
PC4
PC5
Li+Xe
Calorimeter
SPS
Beam pipe

Fig. 1

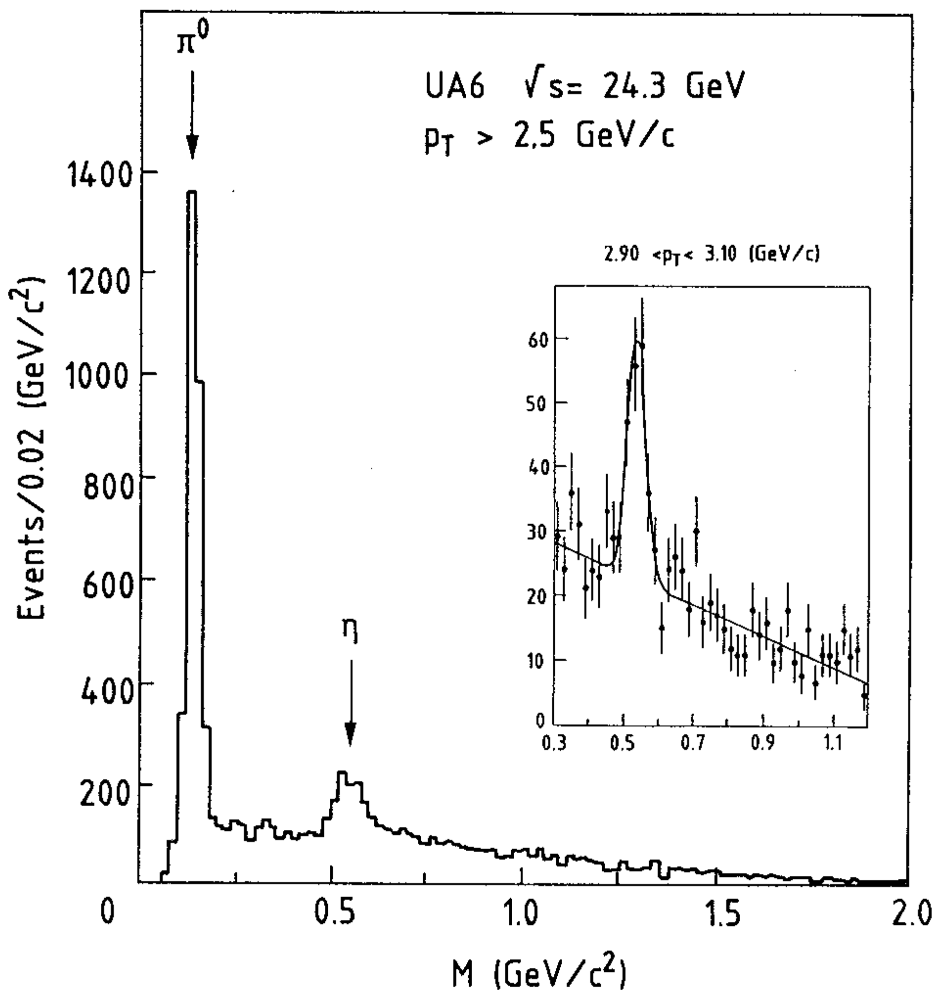
π0
η
UA6 √s= 24.3 GeV
pT > 2,5 GeV/c
2.90 <pT< 3.10 (GeV/c)
Events/0.02 (GeV/c2)
M (GeV/c2)

Fig. 2

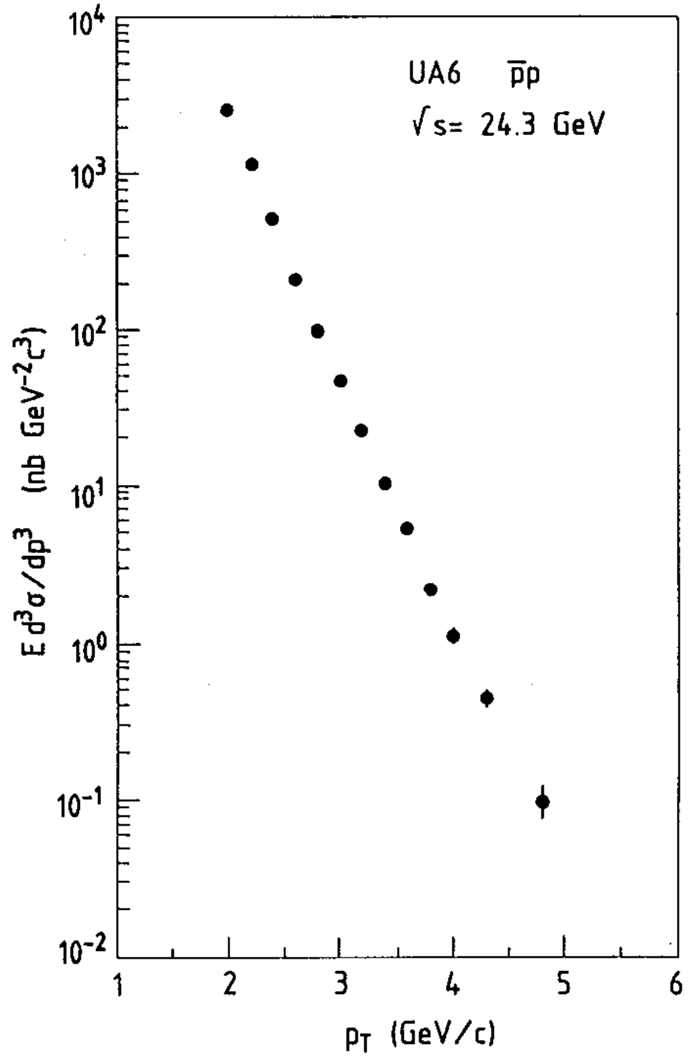
UA6 p̄p
√s= 24.3 GeV
E d3σ/dp3 (nb GeV-2c3)
pT (GeV/c)

Fig. 3

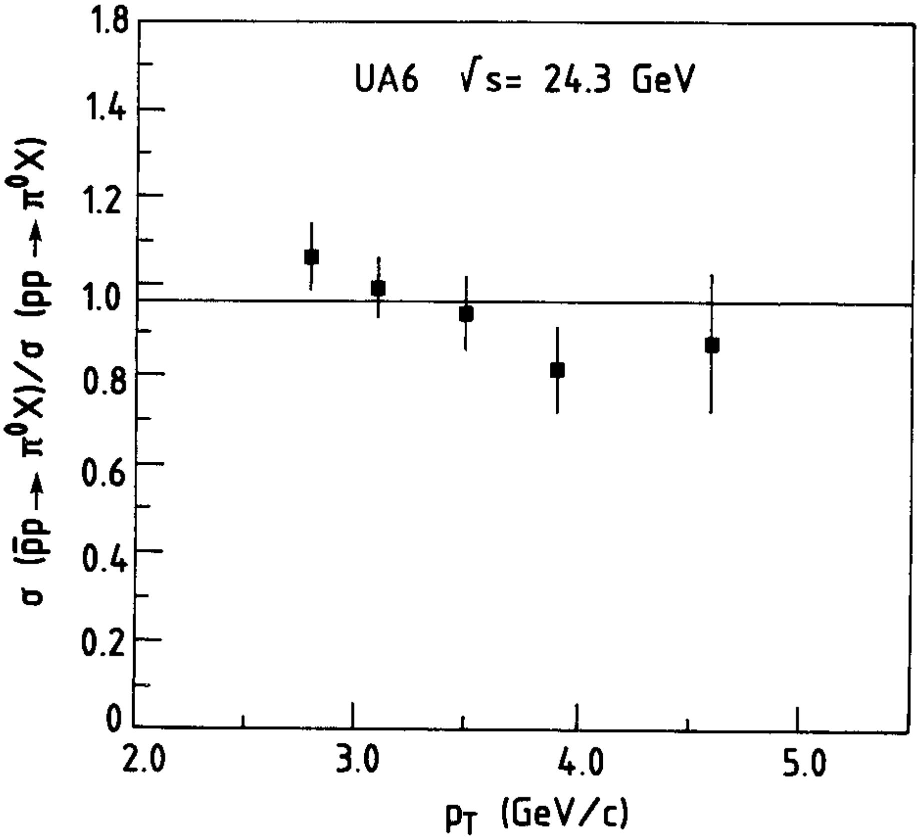

UA6 √s= 24.3 GeV
σ (p̄p → π⁰X)/σ (pp → π⁰X)
1.8
1.4
1.2
1.0
0.8
0.6
0.4
0.2
0
2.0
3.0
4.0
5.0
pT (GeV/c)

Fig. 4

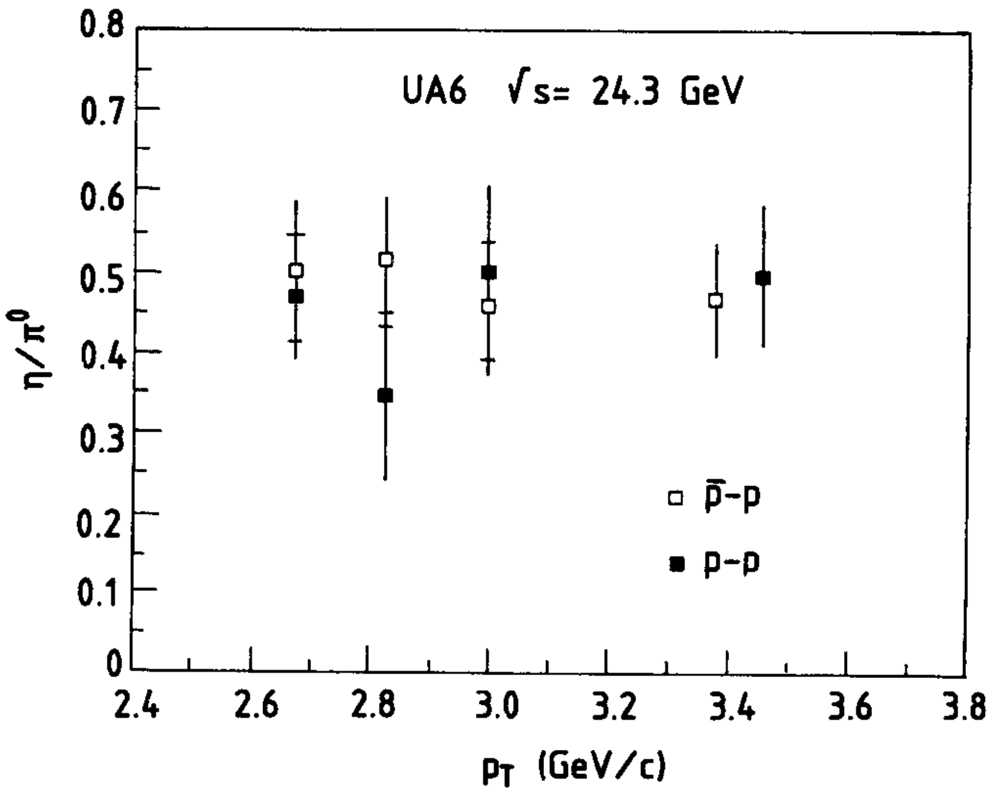

UA6 √s= 24.3 GeV
η/π⁰
0.8
0.7
0.6
0.5
0.4
0.3
0.2
0.1
0
2.4
2.6
2.8
3.0
3.2
3.4
3.6
3.8
pT (GeV/c)
□ p̄-p
■ p-p

Fig. 5